Contribution from the Departments of Chemistry, University of Alberta, Edmonton, Alberta, Canada T6G 2G2, and University of Toledo, 2801 W. Bancroft Street, Toledo, Ohio

Hexacoordinate Phosphorus. 6. Synthesis and Characterization of Neutral Six-Coordinate Phosphorus(V) Compounds Derived from 2-Pyridinol and Related Heteroatomic Pyridine Ligands

Dietmar K. Kennepohl,† A. Alan Pinkerton,‡ Yoke Foo Lee,‡ and Ronald G. Cavell*,†

Received December 27, 1989

The reaction of the silylated form of the substituted pyridine ligands 2-(methylamino)pyridine, 2-hydroxypyridine, 2-mercaptopyridine, and 2,2′-dipyridylamine with λ^5-halogenophosphoranes yields, via trimethylsilyl halide elimination, a series of neutral hexacoordinate λ^6-phosphorus compounds (**1**-**8**), in which a four-membered chelate structure is achieved by donation of the electron pair from the pyridine nitrogen to phosphorus in addition to formation of P–O, P–N, or P–S bonds. The hexacoordinate nature of these compounds is evidenced by their high-field ^{31}P NMR chemical shifts and is further substantiated by the crystal structure of $Cl_4\overline{P(NC_5H_4)}NMe$ (**1**). Crystal data for **1**: orthorhombic, space group $P2_12_12_1$ (No. 19), a = 7.507 (3) Å, b = 11.623 (3) Å, c = 12.577 (2) Å, V = 1097.4 Å^3, Z = 4. Final R and R_w values for **1** are 0.038 and 0.045, respectively. The molecular structure shows also that the methylamino substituent of pyridine lies flat in the radial plane of the molecule, that the exocyclic nitrogen bound to phosphorus is planar, and that both the endocyclic (1.350 (6) Å) and exocyclic (1.344 (6) Å) C–N bond lengths have similar values which are furthermore indicative of C–N multiple bonding. P–Cl bond lengths range from 2.077 to 2.153 Å, with the longest bonds being those perpendicular to the molecular plane and the shortest trans to the donating pyridine nitrogen.

Saturation-transfer NMR experiments indicate that the fluorine exchange in $F_4\overline{P(NC_5H_4)}NMe$ (**2**) involves two competitive processes of the opened-ring intermediate with similar energy barriers of 57.8 (1) (pseudorotation) and 56.1 (1) (ligand rotation) kJ/mol. Synthesis, selected reactions, and NMR spectral characterization of these compounds are reported.

Introduction

Several kinds of neutral λ^6-phosphorus(V) compounds have been structurally characterized recently to provide a substantial list of examples of this previously rare class of compounds. The first examples of the system involved binding of a univalent bidentate ligand such as acetylacetonate (acac)[1,2] or 8-oxyquinolyl[3] to form six-membered-ring chelates including the six-coordinate phosphorus center. Another series based on four-membered-ring structures was defined by our carbamate[4] and thiocarbamate[4] derivatives. Others have prepared several amidine derivatives,[5,6] which also contain a chelated four-membered ring, and the *N*,*N*′-((dimethylamino)acetoxy)phosphorus(V) compounds,[7] which form a chelated five-membered ring. One example of the latter has been structurally characterized.[7] Recently, we have used carbodiimides[8] to build four-membered amidino ring structures incorporating a six-coordinate phosphorus center. In all cases formation of the λ^6-phosphorus center occurs when phosphorus carries strongly electron-withdrawing substituents and so possesses a strong Lewis acid character. The delicate balance which exists between the acid character of the phosphorus and the basic character of the donor means however that the λ^6-phosphorus center may not always be formed.[5-7]

Although bidentate heteroatomic pyridine-based ligands have seen limited use for the preparation of metal chelates and bridges (e.g. use of 2-aminopyridine to form $[H(Ph_3P)_2Ru(HNC_5H_4N)]$, 2-mercaptopyridine to form $[(Ph_3P)_2Ru(SC_5H_4N)_2]$,[9] and 2-hydroxypyridine to form several bimetallic compounds of the type $[M_2(6\text{-methyl-2-hydroxypyridine})_4]$,[10] where M = Mo, Ru, Rh, Pd, and Cr), this ligand system has not been extended to main-group elements. Herein we describe the formation of a new series of neutral six-coordinate phosphorus compounds (Figure 1) using ligands derived from 2-hydroxypyridine and its analogues. The particular feature of interest in these chelated derivatives of P(V) is the formation of a potentially strained four-membered ring. A comparison to the behavior of metals however suggests that the products might have more likely been polymers or λ^5-phosphorus compounds containing monodentate ligands (for example, 2-hydroxypyridine usually serves to bridge dinuclear species or to form polymeric species with metals). There are some exceptions to the general propensity of the metals to form dinuclear or polymeric products, for example, *trans*-$[Ru(6\text{-methyl-2-hydroxypyridine})_2(PPh_3)_2]$.[11] In the present study P(V) formed six-coordinated phosphorus centers with a chelated ligand in all cases.

Table I. Preparation of Silylated 2-Pyridine Derivatives

compd	acid[a] wt, g	CH_3Li (1.4 M) vol, mL	$(CH_3)_3SiCl$ wt, g	yield, %	mp/bp, deg
$Me_3Si(map)$[b]	8.12	56.4	8.79	76	bp 103/0.5 mmHg
$Me_3Si(hp)$	6.54	50.6	8.08	92	bp 97/0.5 mmHg
$Me_3Si(mp)$	7.23	48.9	7.57	68	bp 122/0.5 mmHg
$Me_3Si(dpa)$	9.45	41.1	6.36	83	mp 37-40

[a] Protonated form of the pyridine ligand. [b] Abbreviations: map = 2-(methylamino)pyridinato; hp = 2-hydroxypyridinato; mp = 2-mercaptopyridinato; dpa = 2,2′-dipyridylaminato.

Experimental Section

Starting Materials, General Methods, and Apparatus. The (trifluoromethyl)phosphorane $(CF_3)_3PCl_2$ was prepared by the published method.[12] PCl_5, 2-(methylamino)pyridine, 2-hydroxypyridine, 2-mercaptopyridine, and 2,2′-dipyridylamine were obtained from Aldrich and used without further purification. PF_5 was obtained from Matheson and, as it was found to be free of OPF_3, used without further purification. All solvents were dried and distilled before use. Reaction mixtures

† University of Alberta.
‡ University of Toledo.

(1) Brown, N. M. D.; Bladon, P. *J. Chem. Soc., Chem. Commun.* **1966**, 304. Sheldrick, W. S.; Hewson, M. J. C. *Z. Naturforsch., B: Anorg. Chem.* **1978**, *33B*, 834.
(2) Burford, N.; Kennepohl, D. K.; Cowie, M.; Ball, R. G.; Cavell, R. G. *Inorg. Chem.* **1987**, *26*, 650.
(3) John, K. P.; Schmutzler, R.; Sheldrick, W. S. *J. Chem. Soc., Dalton Trans.* **1974**: (a) 1841; (b) 2466.
(4) Cavell, R. G.; Vande Griend, L. *Inorg. Chem.*: (a) **1986**, *25*, 4699; (b) **1983**, *22*, 2066.
(5) (a) Negrebetskii, V. V.; Kal'chenko, V. I.; Rudyi, R. B.; Markovskii, L. N. *J. Gen. Chem. USSR* (*Engl. Transl.*) **1985**, *55*, 236. (b) Cherkasov, R. A.; Polezhaeva, N. A. *Russ. Chem. Rev.* (*Engl. Transl.*) **1987**, *56*, 163. (c) Added in proof: Markovskii, L.; Kal'chenko, V.; Negrebetskii, V. *New J. Chem.* **1990**, *14*, 339.
(6) (a) Latscha, H. P.; Hormuth, P. B. *Angew. Chem.* **1968**, *81*, 281. (b) Hormuth, P. B.; Latscha, H. P. *Z. Anorg. Chem.* **1969**, *369*, 59. (c) Ziegler, M. L.; Weiss, J. *Angew. Chem., Int. Ed. Engl.* **1969**, *8*, 445.
(7) Krebs, R.; Schmutzler, R.; Schomburg, D. *Polyhedron* **1989**, *8*, 731.
(8) Part 5: Kennepohl, D. K.; Santarsiero, B.; Cavell, R. G. *Inorg. Chem.* preceding paper in this issue.
(9) *Comprehensive Organometallic Chemistry*; Wilkinson, G., Ed.; Pergamon Press: Oxford, England, 1982; Vol. 4, p 725.
(10) Clegg, W.; Garner, C. D.; Al-Samman, M. H. *Inorg. Chem.* **1983**, *22*, 1534.
(11) Clegg, W.; Berry, M.; Garner, C. D. *Acta Crystallogr., Sect. B* **1980**, *36*, 3110.
(12) Bennett, F. W.; Emeleus, H. J.; Haszeldine, R. N. *J. Chem. Soc.* **1953**, 1565.

0020-1669/90/1329-5088$02.50/0

Table II. ^{1}H NMR Chemical Shifts[a] for Silylated Pyridine Ligands

	$Me_3Si(map)$[b]	$Me_3Si(hp)$[c]	$Me_3Si(mp)$[b]	$Me_3Si(dpa)$[c]
$(CH_3)_3Si$	0.045 s[d,e]	0.30 s	0.21 s	0.25 s
	6.55 d	7.00–7.25 m	6.94 br tr	6.55 d
pyridine	6.66 d/d		7.26 d	6.86 br tr
ring	7.53 d/tr	7.80 br tr	7.41 br tr	7.54 d/tr
protons	8.21 d/d	8.45 br d	8.30 br s	8.41 br d

[a] Chemical shifts in ppm vs TMS. [b] Determined with 400-MHz instrument. [c] Determined with 80-MHz instrument. [d] Abbreviations: s = singlet; d = doublet; tr = triplet; m = multiplet; br = broad. [e] CH_3 protons on N at 2.92 ppm.

prepared under vacuum conditions were typically degassed by means of two or three freeze–thaw cycles before the combination of the reagents was allowed to react. The ^{1}H, ^{19}F, and ^{31}P NMR spectra were obtained using Bruker WP200, WP80, and WP400 spectrometers on $CDCl_3$ solutions (approximately 10% compound) in vacuum-sealed 5-mm NMR tubes. Mass spectra were recorded with AEI MS-12 and MS-50 spectrometers operating at an ionizing voltage of 70 eV. All manipulations were carried out either in vacuum or under dry argon. Melting points were recorded on samples sealed in a glass melting point tube and are uncorrected.

General Synthesis of the Silylated Pyridine Derivatives. A weighed sample of pyridinol, thiol, or amine was placed in a 500-mL round-bottom flask and dissolved in 200 mL of diethyl ether. The solution was stirred and cooled in an ice bath. A diethyl ether solution of CH_3Li (1.4 M) was added dropwise over a period of 1 h. The solution was warmed to room temperature for 2 h and then cooled again in an ice bath. An equivalent amount of $(CH_3)_3SiCl$ was added dropwise for 0.5 h. The solution was warmed to room temperature and left to stir for an additional 3 h. The white precipitate that formed was filtered by using a C glass frit and the diethyl ether was removed by using a rotary evaporator. Distillation of the remaining liquid (solid in the case of 2,2′-dipyridyl-(trimethylsilyl)amine preparation) using a 15-cm, vacuum-jacketed, Vigreux column afforded pure product. The details of each preparation are given in Table I, and the NMR spectral results are given in Tables II and III.

Synthetic Procedure A for the Tetrachlorophosphorus Products. A sample of the trimethylsilylated pyridine ligand was placed in a round-bottom flask and dissolved in CCl_4. An equivalent amount of PCl_5 was dissolved in CCl_4, and this PCl_5 solution was added directly to the trimethylsilylated pyridine ligand solution at room temperature. A precipitate formed immediately on mixing the reagents. The solution was stirred under Ar for several hours to ensure complete reaction. The solvent was then removed under vacuum to leave a solid.

Synthetic Procedure B for the Tetrafluoro- and (Trifluoromethyl)-phosphorus Products. A sample of trimethylsilylated pyridine ligand was placed in a small glass reaction vessel and degassed three times by using a freeze–thaw cycle. Then 3 mL of $CFCl_3$ was cryogenically distilled in,

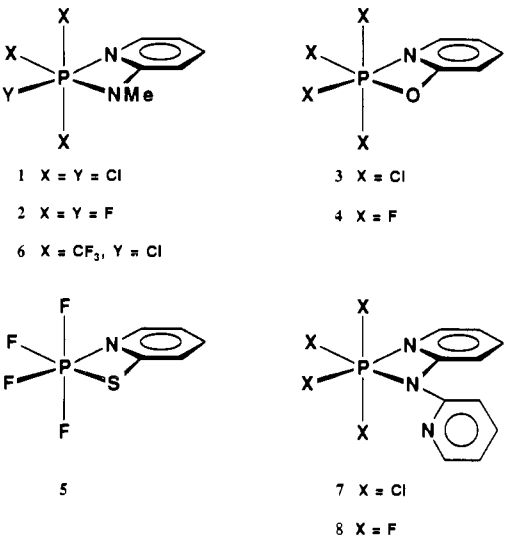

Figure 1. Structures of heteroatom pyridine λ^6-phosphorus compounds (**1–8**).

followed by a sample of the phosphorane (1 equiv). The vessel was flame-sealed under vacuum and allowed to warm to room temperature over a period of 3 h whereupon a white precipitate formed. The glass reaction vessel was opened under vacuum with a Stock-breaker and the volatile materials were pumped away, to leave a solid product. Yields were 90% or greater.

(2-(Methylamino)pyridinato)tetrachlorophosphorus(V) (1). General preparation A (conducted on a 7.75-mmol scale) gave a yellow solid (mp 167–172 °C). Anal. Calcd for $C_6H_7Cl_4N_2P$: C, 25.74; H, 2.52; Cl, 50.66; N, 10.01. Found: C, 25.57; H, 2.39; Cl, 48.35; N, 9.92. MS (*m/e* (relative intensity, % of strongest peak), identity): 280 (7.5), M; 243 (100), M – Cl; 208 (41.9), M – 2Cl; 173 (54.1), PCl_4; 137 (5.3), PCl_3; 107 (92.9), $NC_5N_4NCH_3$; 78 (11.3), NC_5H_4.

(2-(Methylamino)pyridinato)tetrafluorophosphorus(V) (2). General preparation B (from PF_5 conducted on a 3.5-mmol scale) gave a white solid (mp 105–108 °C). Anal. Calcd for $C_6H_7F_4N_2P$: C, 33.66; H, 3.30; N, 13.08. Found: C, 33.34; H, 3.46; N, 12.70. MS (*m/e* (relative intensity, % of strongest peak), identity): 214 (24.1), M; 195 (16.8), M – F; 107 (100), PF_4; 92 (2.1), NC_5H_4N; 79 (22.6), NC_5H_5.

Tetrachloro(2-hydroxypyridinato)phosphorus(V) (3). General preparation A (conducted on a 10.5-mmol scale) gave a white solid (mp 123–125 °C). Anal. Calcd for $C_5H_4Cl_4NOP$: C, 22.50; H, 1.51; Cl, 53.14; N, 5.25. Found: C, 24.37; H, 1.85; Cl, 48.01; N, 5.62. MS (*m/e* (relation intensity, % of strongest peak), identity): 232 (21.2), M – Cl; 173 (19.3), PCl_4; 160 (20.2), M – 3Cl; 101 (10.7), PCl_2; 78 (100), NC_5H_4; 66 (96), PCl.

Table III. NMR Parameters for Compounds **1–8** and F_5P·py

cmpd[a]	$\delta(^1H)$[b]	$\phi(^{19}F)$[c]	$\sigma(^{31}P)$[d]	$^3J_{PH(A)}$, Hz	$^1J_{PF(ax)}$, Hz	$^1J_{PF(rad)}$, $^1J'_{PF(rad)}$, Hz	other couplings, Hz
1	8.20[e]		−195.7	17			$^3J_{PH(Me)}$ = 27
	3.31[f]						
2	7.60–7.74[e,j]	−70.9 (2)[g,h]	−132.4[i]	*j*	827	838 (862)	$^2J_{F(ax)F(rad)}$ = 60
	2.29[f]	−73.8 (1)[i]					$^2J_{F(ax)F'(rad)}$ = 65
		−89.0 (1)[i]					$^2J_{F(rad)F'(rad)}$ = 68
3	8.33[e]		−184.5	16			
4	8.03[e]	*k*	−131.3[p]	13.6	855[l]		
5	8.12[e]	−117.8 (2)[h]	−136.4[i]	14.5	968	747 (1002)	$^2J_{F(ax)F(rad)}$ = 47
		−134.7 (1)[i]					$^2J_{F(ax)F'(rad)}$ = 83
		−159.3 (1)[i]					$^2J_{F(rad)F'(rad)}$ = 55
6	7.75–7.85[e,j]	−62.0 (1)[m]	−152.2[o]	*j*			$^2J_{PF(rad)}$ = 91
	3.22[j]	−67.2 (2)[n]					$^2J_{PF(ax)}$ = 118
							$^2J_{FF}$ = 14
7	8.48[e]		−202.2	15.5			
8	8.12–8.20[e,j]	−63.6 (2)[h]	−135.3[i]	*j*	835	829 (864)	$^2J_{F(ax)F(rad)}$ = 58
	−75.4 (1)[i]						$^2J_{F(ax)F'(rad)}$ = 63
	−79.1 (1)[i]						$^2J_{F(rad)F'(rad)}$ = 67
F_5P·py			−144.2[q,r]	6.8	788[s] (cis)	759[s] (trans)	

[a] In $CDCl_3$. [b] ppm relative to TMS. [c] ppm relative to $CFCl_3$. [d] ppm relative to 85% H_3PO_4. [e] Pyridine ring α proton. [f] Methyl group on amine. [g] At −50 °C. [h] Doublet of doublets of doublets. [i] Doublet of doublets of triplets. [j] Obscured by overlapping multiplets. [k] Very broad signals. [l] Average value; fluorines fluxional. [m] Doublet of septets. [n] Doublet of quartets. [o] Septet of quartets. [p] Pentet of broad lines. [q] Hexet of broad lines. [r] At 22 °C. [s] John, K.-P.; Schmutzler, R. *Z. Naturforsch.* **1974**, *29B*, 730.

Table IV. Crystal Data and Details of Intensity Collection for Cl_4P(map) (**1**)

mol formula	$C_6H_7Cl_4N_2P$
fw	279.92
space group	orthorhombic, $P2_12_12_1$ (No. 19)
temp, °C	−20 (1)
radiation (λ, Å)	Mo Kα (0.71073)
unit cell params	
a, Å	7.507 (3)
b, Å	11.623 (3)
c, Å	12.577 (2)
V, Å^3	1097.4
Z	4
ρ_{calcd}, g cm^{-3}	1.69
linear abs coeff μ, cm^{-1}	11.9
final R, R_w, GOF[a]	0.038, 0.045, 1.47

[a] $R = \sum||F_o| - |F_c||/\sum|F_o|$; $R_w = [\sum w(|F_o| - |F_c|)^2/\sum wF_o^2]^{1/2}$; GOF $= [\sum w(|F_o| - |F_c|)^2/(NO - NV)]^{1/2}$.

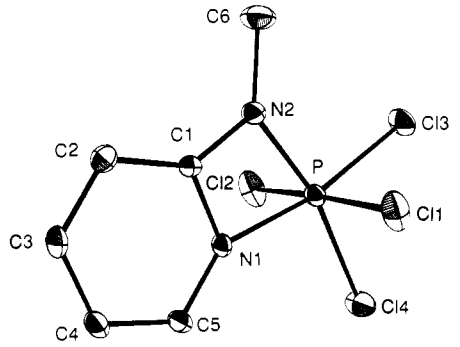

Figure 2. Perspective view of **1**, showing atom-labeling scheme. All non-hydrogen atoms are represented by Gaussian ellipsoids at the 20% probability level.

Tetrafluoro(2-hydroxypyridinato)phosphorus(V) (4). General preparation B (from PF_5 conducted on a 6-mmol scale) gave a white solid (mp 83–85 °C). Anal. Calcd for $C_5H_4F_4NOP$: C, 29.87; H, 2.01; N, 6.97. Found: C, 29.67; H, 1.96; N, 6.86. MS (*m/e* (relative intensity, % of strongest peak), identity): 201 (16.7), M; 182 (1.4), M − F; 107 (100), PF_4; 95 (16.6), NC_5H_4O; 78 (13.3), NC_5H_4; 64 (11.2), C_5H_4.

Tetrafluoro(2-mercaptopyridinato)phosphorus(V) (5). General preparation B (from PF_5 conducted on a 3-mmol scale) gave a yellow solid (mp 95–99 °C). Anal. Calcd for $C_5H_4F_4NPS$: C, 23.24; H, 1.97; N, 6.83. Found: C, 23.42; H, 1.72; N, 6.80. MS (*m/e* (relative intensity, % of strongest peak), identity): 187 (17.0), M − F; 142 (6.3), NC_5H_4SP; 107 (100), PF_4; 78 (41.6), NC_5H_4; 69 (15.1), PF_2.

Chloro(2-(methylamino)pyridinato)tris(trifluoromethyl)phosphorus(V) (6). General preparation B (from $(CF_3)_3PCl_2$ conducted on a 0.35-mmol scale) gave a white solid (mp 105–108 °C). Anal. Calcd for $C_9H_7F_9ClN_2P$: C, 28.40; H, 1.85; N, 7.36. Found: C, 29.97; H, 2.04; N, 7.56. MS (*m/e* (relative intensity, % of strongest peak), identity): 380 (3.7), M; 365 (10.4), M − CH_3; 345 (41.5), M − Cl; 311 (100), M − CF_3; 295 (11.3), $C_2F_6ClPNC_5H_3N$; 273 (6.0), C_3F_9ClP; 261 (25.7), $C_2F_6PNC_5H_4N$; 228 (12.9), $CF_3ClPNC_5H_4N$; 137 (17.7), $PNC_5H_4NC-H_2$; 107 (19.5), $NC_5H_4NCH_3$; 78 (72.2), NC_5H_4; 69 (38.8), PF_2.

(2,2′-Dipyridylaminato)tetrachlorophosphorus(V) (7). General preparation A (conducted on a 4.8-mmol scale) gave a yellow solid (mp 163–166 °C). Anal. Calcd for $C_{10}H_8Cl_4N_3P$: C, 34.82; H, 2.92; Cl, 41.10; N, 12.18. Found: C, 35.10; H, 2.62; Cl, 39.63; N, 12.22. MS (*m/e* (relative intensity, % of strongest peak), identity): 306 (12.6), M − Cl; 271 (9.0), M − 2Cl; 236 (72.2), M − 3Cl; 200 (14.4), M − 4Cl; 170 (100), $NC_{10}H_8N_2$; 122 (43.3), PNC_5H_4N; 101 (41.7), PCl_2; 78 (77.7), NC_5H_4.

(2,2′-Dipyridylaminato)tetrafluorophosphorus(V) (8). General preparation B (from PF_5 conducted on a 1.6-mmol scale) gave a white solid (mp 77–79 °C). Anal. Calcd for $C_{10}H_8F_4N_3P$: C, 43.34; H, 2.91; N, 15.16. Found: C, 41.92; H, 2.89; N, 14.61. MS (*m/e* (relative intensity, % of strongest peak), identity): 277 (100), M; 258 (8.6), M − F; 170 (90.4), $NC_{10}H_8N_2$; 107 (79.2), PF_4; 92 (2.5), NC_5H_4N; 78 (50.8), NC_5H_4; 51 (18.7), C_4H_3.

Crystallography. A yellow crystal of $C_6H_7Cl_4N_2P$ (**1**), having an irregular shape with the approximate dimensions of 0.10 × 0.35 × 0.36 mm, was mounted in a capillary under argon. Preliminary examination and data collection were performed with Mo Kα radiation (λ = 0.71073 Å; graphite monochromator) on an Enraf-Nonius CAD4 diffractometer at −20 (1) °C. Orthorhombic cell constants were obtained from the setting angles of 25 reflections ($10 < \theta < 12°$),[13a] and the space group ($P2_12_12_1$, No. 19) was uniquely defined by systematic absences.[13a] ω

Table V. Positional[a] and Thermal Parameters of All Non-Hydrogen Atoms for Cl_4P(map) (**1**)

atom	x	y	z	B,[b] Å^2
P	4768 (2)	546 (1)	1011 (1)	2.70 (3)
Cl(1)	1901 (2)	521 (1)	962 (2)	4.76 (4)
Cl(2)	7611 (2)	499 (2)	1110 (2)	5.56 (5)
Cl(3)	4770 (2)	2324 (1)	1172 (1)	4.19 (3)
Cl(4)	4628 (4)	139 (1)	2638 (1)	5.41 (5)
N(1)	4784 (6)	−970 (3)	574 (3)	2.49 (9)
N(2)	4841 (8)	497 (4)	−390 (3)	3.4 (1)
C(1)	4829 (8)	−657 (4)	−459 (4)	2.7 (1)
C(2)	4850 (9)	−1490 (5)	−1249 (4)	3.7 (1)
C(3)	4779 (9)	−2608 (5)	−917 (4)	4.1 (1)
C(4)	4720 (10)	−2909 (4)	140 (5)	4.0 (1)
C(5)	4719 (8)	−2072 (4)	892 (4)	3.4 (1)
C(6)	4880 (10)	1319 (5)	−1236 (5)	4.8 (2)

[a] Values × 10^4. [b] Anisotropically refined atoms are given in the form of the isotropic equivalent displacement parameter defined as $8\pi^2/3 \times$ Tr (orthogonalized **U** tensor).

Table VI. Selected Bond Distances and Angles for Cl_4P(map) (**1**)

Bond Distances[a]			
P–Cl(1)	2.153 (2)[b]	N(1)–C(5)	1.343 (6)
P–Cl(2)	2.139 (2)	N(2)–C(1)	1.344 (6)
P–Cl(3)	2.077 (2)	N(2)–C(6)	1.430 (7)
P–Cl(4)	2.103 (2)	C(1)–C(2)	1.388 (7)
P–N(1)	1.845 (4)	C(2)–C(3)	1.366 (8)
P–N(2)	1.763 (4)	C(3)–C(4)	1.375 (8)
N(1)–C(1)	1.350 (6)	C(4)–C(5)	1.357 (7)
Bond Angles[c]			
Cl(1)–P–Cl(2)	177.2 (1)[b]	N(1)–P–N(2)	70.9 (2)
Cl(1)–P–Cl(3)	90.96 (9)	P–N(1)–C(1)	91.7 (2)
Cl(1)–P–Cl(4)	88.6 (1)	P–N(1)–C(5)	145.2 (4)
Cl(1)–P–N(1)	89.2 (2)	C(1)–N(1)–C(5)	123.0 (4)
Cl(1)–P–N(2)	90.2 (2)	P–N(2)–C(1)	95.5 (3)
Cl(2)–P–Cl(3)	91.07 (9)	P–N(2)–C(6)	136.3 (4)
Cl(2)–P–Cl(4)	89.3 (1)	C(1)–N(2)–C(6)	128.2 (4)
Cl(2)–P–N(1)	89.2 (2)	N(1)–C(1)–N(2)	101.9 (4)
Cl(2)–P–N(2)	91.5 (2)	N(1)–C(1)–C(2)	120.1 (4)
Cl(3)–P–Cl(4)	97.39 (9)	N(2)–C(1)–C(2)	137.9 (5)
Cl(3)–P–N(1)	168.3 (2)	C(1)–C(2)–C(3)	116.4 (5)
Cl(3)–P–N(2)	97.4 (2)	C(2)–C(3)–C(4)	122.6 (5)
Cl(4)–P–N(1)	94.3 (1)	C(3)–C(4)–C(5)	119.4 (5)
Cl(4)–P–N(2)	165.2 (2)	N(1)–C(5)–C(4)	118.4 (5)

[a] In angstroms. [b] Numbers in parentheses are estimated standard deviations in the least significant digits. [c] In degrees.

Table VII. M_z Values and Time for Three Fluorine Sites in **2**

time, s	$M_z(F_{ax})$[a]	$M_z(F_{rad})$[a]	$M_z(F'_{rad})$[a]
0.001	406.22	193.03	−152.78
0.002	400.75	194.06	−128.67
0.004	395.87	194.06	−143.34
0.010	397.80	183.79	−125.68
0.020	383.05	175.73	−90.35
0.040	377.32	160.44	−64.39
0.100	350.14	129.27	22.49
0.200	330.74	119.36	77.27
0.400	312.05	125.83	119.42
0.600	315.60	147.27	147.37
1.000	344.13	172.25	168.31
2.000	382.94	200.63	190.22
5.000	409.16	217.19	207.40

[a] *z* magnetization in arbitrary units.

(13) (a) The diffractometer programs are those supplied by Enraf-Nonius for operation of a CAD4F diffractometer. (b) *International Tables for X-ray Crystallography*; Kynoch Press: Birmingham, England, 1974; Vol. I. (c) Cromer, D. T.; Waber, J. T. *Ibid.*; Vol. IV, Table 2.2B. (d) *Ibid.*; Table 2.3.1. (e) Frenz, B. A. In *The Enraf-Nonius CAD4SDP-A Real-time System for Concurrent X-Ray Data Collection and Crystal Structure Determination in Computing in Crystallography*; Schenk, H.; Olthof-Hazelkamp, R., van Konigsveld, H., Bassi, G. C., Eds.; Delft University Press: Delft, Holland, 1978; pp 64–71.

scans of several intense reflections indicated good crystal quality. The 1275 unique intensities (ω–2θ scans) were corrected for absorption and decay. The crystal data, measurement methods, structure solution, and refinement are summarized in Table IV. The structure was solved by direct methods and refined on F in full-matrix least squares to $R = 0.037$ and $R_w = 0.045$. Hydrogen atoms were included in the refinement with isotropic thermal parameters, but three of them were restrained to ride on the atom to which they are bonded. Scattering factors were taken from Cromer and Waber,[13b] and anomalous dispersion coefficients were those of Cromer.[13d] All calculations were carried out on a VAX 11/750 computer using SDP/VAX[13e] software. Final atomic parameters for compound **1** are reported in Table V, and selected derived bond lengths and angles, in Tables VI and VII. A perspective view of the molecule is given in Figure 2. A complete structure report including tables of observed and calculated structure factors, anisotropic temperature factors, bond lengths and angles is available as supplementary material.

Determination of the Energy Barrier for Fluorine Exchange in 2. Free energy of activation (ΔG^*) for the fluorine exchange process in **2** was determined by means of two NMR double-resonance techniques. The spin-saturation-transfer (SST) experiment was carried out on a Bruker WP400 spectrometer at 243 K (−30 °C). The axial fluorines were saturated at −69.9 ppm, causing partial saturation of the radial fluorines. The spin–lattice relaxation times (T_1) of the radial fluorines were determined by standard methods.[14a,b] The two rate constants for two-site axial–radial fluorine exchange at −30 °C were calculated with eq 1, where M_z^∞ is the equilibrium magnetization with saturation at another site and M_z^0 is the normal magnetization without saturation.

$$k = \frac{1}{T_1}\left[\frac{M_z^0 - M_z^\infty}{M_z^\infty}\right] \quad (1)$$

An average rate constant was derived from the two individual rate constants, and from that value eq 2 was applied to yield a ΔG^* of 56.4 (5) kJ/mol at −30 °C.

$$\Delta G^* = -RT \ln k\left(\frac{Nh}{RT}\right) \quad (2)$$

Further study of the system by means of a selective-inversion-transfer (SIT) experiment was carried out on a Bruker WP400 spectrometer at 243 K (−30 °C). In this case selective inversion of the upfield radial fluorine (F'_{rad}) at −89.0 ppm was applied and the temporal response of z magnetization (M_z) at the other two sites (F_{ax} and F_{rad}) was observed during an evolution period. The pulse sequence

relaxation delay–selective 180° pulse–τ–
nonselective 90° pulse–acquisition

was repeated for a series of τ values, where $0 \le \tau \le 5T_1$. The computer program developed by Muhandiram and McClung[14c,d] was used to fit the data to rate constants for proposed mechanisms. The best fit was found for a mixture of two exchange processes that may occur in the five-coordinate F_4PL species with the monodentate substituent. These are described by the rate constants k_1 for pseudorotation fluorine exchange and k_2 for simple rotation about the P–N bond to interchange radial fluorines, respectively. The two individual energy barriers to fluorine exchange in compound **2** were separately calculated by using eq 2 and fitted separately and in combination. The best fit corresponded to a combination of the energy barrier for pseudorotational fluorine exchange (ΔG_1^* = 57.8 (1) kJ/mol) and for rotational radial fluorine exchange (ΔG_2^* = 56.1 (1) kJ/mol) at −30 °C.

Results and Discussion

Silylated heteroatom pyridines were readily prepared from the commercially available protonated form of the ligands via a conventional lithiation followed by reaction with $(CH_3)_3SiCl$ (eq 3). These silylated derivatives react readily with a λ^5-phosphorane to give high yields (typically 80–90%) of the λ^6-phosphoranes (**1**–**8**)


(3a)


(3b)

E = NCH_3, O, S, NPy

in eq 4. Similar smooth reactions of fluorophosphoranes with

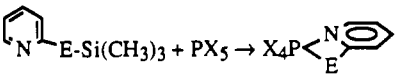
(4)

X = F, Cl, CF_3; E = NCH_3, O, S, NPy

(Figure 1) via elimination of $(CH_3)_3SiCl$ or $(CH_3)_3SiF$ as shown the analogous 8-(trimethylsiloxy)quinoline and (*N*,*N*′-dimethylaminoacetoxy)trimethylsilane have been reported recently.[7] These reactions gave either λ^5- or λ^6-phosphorus chelates according to the nature of the substituents on phosphorus. Attempts to form bicyclic six-coordinate P(V) derivatives via a similar procedure with disilylated ligands gave only one example of a λ^6-phosphorus compound, $F_3P(OC_2H_4)_2S$;[15] all other final products were anions.

The chlorine-containing compounds formed here (**1**, **3**, **6**, **7**) and our chlorinated amidines $Cl_4PN(R)CN(R)$[8] and $Cl_4PN(Me)C(Cl)N(Me)$[6] are the only examples of stable neutral λ^6-phosphorus compounds containing chlorine substituents. Attempts to form a λ^6-chlorophosphorus compound with carbamate ligands gave only a λ^4 (P=O) product,[3] and exploratory reactions of chloro(trifluoromethyl)phosphoranes with acac did not produce identifiable chlorinated λ^6-P (acac) compounds.[16] The isolation of these chlorinated pyridinol and amidino[8] λ^6-phosphorus compounds indicates, as might be expected, that the chlorine-substituted systems are not inherently unstable. Successful synthesis of the chlorides however requires that any facile transformation pathway that can generate a λ^4-P(V) product be blocked.

The chlorinated compounds **1**, **3**, **6**, and **7** can also be obtained from the direct reaction of a λ^5-chlorophosphorane and the protonated form of the ligand by elimination of HCl under conditions of simple reflux in CCl_4 (eq 5). However, in comparison to the

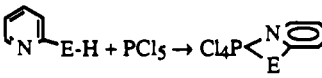
(5)

reactions of the silylated ligands, this method was slow and the reaction was more complex because of the interference of side reactions of the generated HCl. Typical problems include reaction of the nitrogen of the pyridine ring in **1**, **3**, **6**, and **7** or the nitrogen of the amino group (in **1**, **6**, and **7**) with HCl to form stable ammonium chloride salts in the product mixture (eqs 6 and 7),

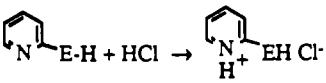
(6)

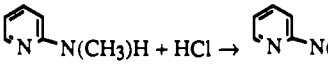
(7)

which results in separation problems. In the reactions with fluorophosphoranes, free HF reacts with PF_5 to form $H^+PF_6^-$ that is difficult to separate from the target compound. Use of silyl reagents to form **2**, **4**, and **5** alleviated this complication. As a result of these complications, we did not find reactions of phosphorus(V) halides with the protonated form of the ligands to be effective routes to desired products and so details are not reported here.

An attempt was made to prepare a chloro analogue of **5** to complete the series. Neither of the reactions of PCl_5 with the

(14) (a) Derome, A. E. *Modern nmr Techniques for Chemistry Research*; Pergamon: London, 1987. (b) Vold, R. L.; Waugh, J. S.; Klein, M. P.; Phelps, D. E. *J. Chem. Phys.* **1968**, *48*, 3831. (c) Muhandiram, D. R.; McClung, R. E. D. *J. Magn. Reson.* **1987**, *71*, 187 and references therein. (d) The program for SIT analysis was provided to us by Drs. Muhandiram and McClung, and calculations were done by Mrs. G. Aarts, Department of Chemistry, University of Alberta.
(15) Robert, D.; Gawad, H. A.; Reiss, J. G. *Bull. Soc. Chim. Fr.* **1987**, 511.
(16) Burford, N.; Cavell, R. G. Unpublished observation.
(17) Pauling, L. *The Nature of the Chemical Bond*, 3rd ed.; Cornell University Press: Ithaca, NY, 1960.
(18) Sheldrick, W. S. *J. Chem. Soc., Dalton Trans.* **1974**, 1402.

protonated or the silylated forms of 2-mercaptopyridine afforded the desired product, $Cl_4P(mp)$ (mp = 2-mercaptopyridinato).

Compounds **1–8** are white or light yellow thermally stable, but moisture sensitive, solids (mp 80–170 °C). In all cases substitution at E was accompanied by coordination of the pyridine nitrogen to the Lewis acid phosphorus center to form a neutral molecule with a six-coordinate phosphorus center, so it is clear that the phosphorus is sufficiently acidic and/or the pyridine nitrogen sufficiently basic for complete or almost complete bidentate binding to occur.

Structure of $Cl_4P(map)$ (1) (map = 2-(Methylamino)-pyridinato). The structure of **1**, shown in Figure 2, shows clearly the hexacoordinate environment around phosphorus. Relevant metrical parameters for **1** are given in Tables VI and VII.

Similar to other λ^6-phosphoranes containing a chelated ligand forming a four-membered ring, such as dimethylcarbamate[4a] or chloroamidino[8] substituents, **1** deviates from ideal octahedral geometry around phosphorus. The tight four-membered ring subtends a very small angle at phosphorus in **1** (70.9 (2)°). This angle is almost the same as that in $Cl_2(CF_3)_2\overline{PN(R)C(Cl)N(R)}$ (R = cyclohexyl),[8] and the result of this compression is to allow more room for the chlorine atoms to spread out around the phosphorus in the radial plane. The Cl(3)–P–Cl(4) angle of 97.39 (9)° is therefore substantially larger than the 90° angle required for an ideal octahedral arrangement. The four chlorine atoms around phosphorus also bend slightly away from the methylamino group and toward the pyridine ring with a Cl(1)–P–Cl(2) angle of 177.2 (1)°. This is presumably a result of greater steric demand generated by the methyl group on N(2) compared to the planar geometry of atoms around the pyridine nitrogen (N(1)). The P–Cl bond distances range from 2.077 (2) to 2.153 (2) Å. The two longest bonds are those perpendicular to the molecular plane. The P–N(2) bond distance of 1.763 (4) Å is only slightly shorter than that expected for a P–N single bond estimated from covalent radii (1.78 Å),[17] and the bond distance of 1.845 (4) Å from phosphorus to the ring nitrogen (P–N(1)) is comparatively long in keeping with the formal structure of **1**, with a single covalent P–N(2) σ bond and a dative bond between P and N(1). The P–N(1) dative bond length here is shorter than the P–N dative bond length for the base adduct $F_5P{\cdot}py$[18] (1.899 Å) but is similar to that found for $F_5P{\cdot}NH_3$[19] (1.849 Å). The dative P–N bond lengths in the chelated systems F_4P(8-oxyquinolyl) (1.191 Å),[3] PhF_3P(8-oxyquinolyl) (1.980 Å),[3] and $PhF_3\overline{P(OC(O)CH_2NMe_2)}$ (2.013 Å)[7] are considerably longer than the dative bond shown by **5**, so in the present case this bond appears to be stronger (more covalent in character) than those chelate distances encountered previously.

Other features of the geometry are also notable. The bond distances within the pyridine ring and the N(2)–C(6) single-bond distance in the methylamino group are normal. There is a planar arrangement of the directly bound atoms C(1), C(6), and P around N(2). The C(1)–N(2) (1.344 (6) Å) and C(1)–N(1) (1.350 (6) Å) bond distances in the chelating ring are significantly shorter than distances expected for a typical C–N single bond (1.45 Å) and are both comparable to the partial C–N double-bond distance (1.310 Å) found in $Cl_2(CF_3)_2\overline{PN(R)C(Cl)N(R)}$ (R = cyclohexyl).[8] Double-bond character is to be expected for C(1)–N, because it is part of the pyridine ring system, but the short C(1)–N(2) length along with the planarity of N(2) indicates that there is a substantial exocyclic delocalization involving N(1)–C(1)–N(2) to form a bidentate anion. The radial P–Cl bond distances are both shorter than the axial P–Cl bonds, and these radial bonds differ in accord with differing trans influences from the two nitrogens; the shorter P–Cl(3) bond (2.077 (2) Å) is trans to the heterocyclic ring donor nitrogen N(1), and the longer P–Cl(4) bond distance (2.103 (2) Å) is trans to the σ-bound N(2) amine nitrogen. Finally, we note the extended planarity of the molecule. All the atoms, with the exception of the axial chlorines (Cl(1) and Cl(2)) and the methyl hydrogens, are coplanar. The largest deviation from the plane occurs at N(1), which sits 0.026 (5) Å below the least-squares plane formed by all these atoms. This extended planarity is of course a reflection of the formation of the bidentate delocalized anionic structure by atoms N(1)–C(1)–N(2)–P and C(6) and incorporates the pyridine ring.

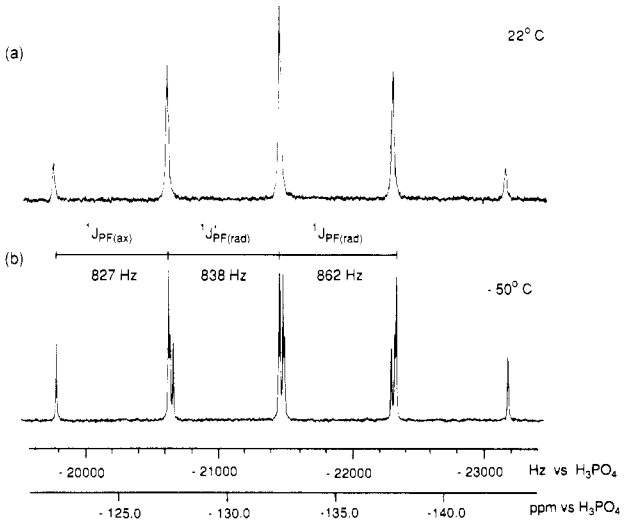

Figure 3. $^{31}P\{^1H\}$ NMR (161.8 MHz) spectra of **2** at (a) 22 °C and (b) −50 °C in $CDCl_3$ solution.

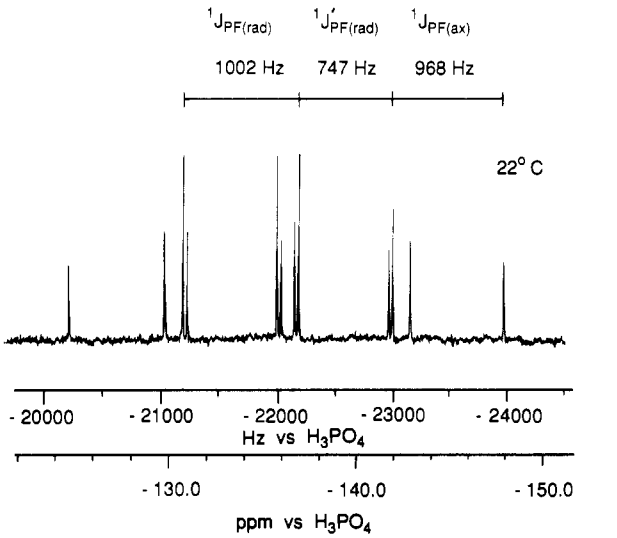

Figure 4. $^{31}P\{^1H\}$ NMR (161.8 MHz) spectrum of **5** in $CDCl_3$ solution at 22 °C.

Nuclear Magnetic Resonance Spectra. The structure and stereochemistry of all of our heteroatom pyridine substituted phosphorus compounds can be readily deduced from their ^1H, ^{19}F, and ^{31}P NMR spectra, and examples are illustrated in Figures 3–5. A summary of the NMR parameters of **1–8** is given in Table III. Although most of these λ^6-phosphoranes are not fluxional at ordinary probe temperatures, some required cooling to obtain the limiting spectrum indicative of the six-coordinate form of the compound. In all cases the low-frequency ^{31}P NMR chemical shifts (−131.3 to −202.2 ppm) that were characteristic of a hexacoordinate phosphorus center were observed even in the fluxional cases.

The tetrachloro compounds (**1**, **3**, and **7**) were immediately identified as λ^6-phosphorus derivatives by ^{31}P NMR spectroscopy in solution by their low-frequency shifts and characteristic couplings to the protons on the chelating ligand. For example, **1** resonates at −195.7 ppm, which is a substantially lower chemical shift value than that displayed by its precursor, PCl_5 (−80 ppm).[20]

(19) Storzer, W.; Schomburg, D.; Roschenthaler, G.-V.; Schmutzler, R. *Chem. Ber.* **1983**, *116*, 367.

(20) Emsley, J. W.; Feeney, J.; Sutcliffe, L. H. *High Resolution Nuclear Magnetic Resonance Spectroscopy*; Pergamon Press: New York, 1966; p 1151.

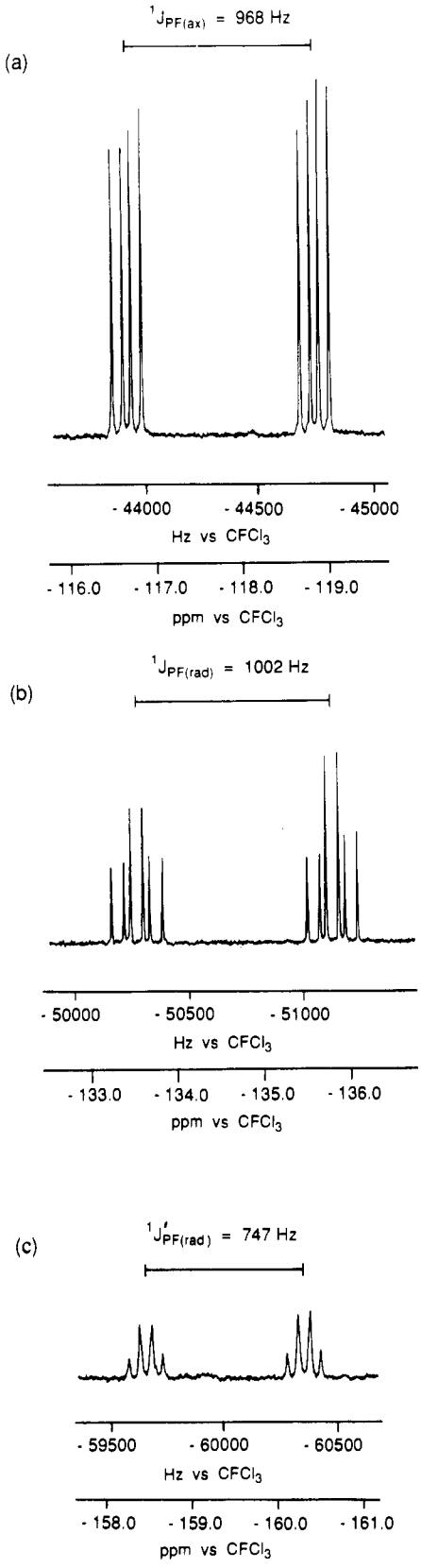

Figure 5. ^{19}F NMR (376.5 MHz) spectra of **5** in $CDCl_3$ solution showing (a) axial, (b) radial, and (c) radial' fluorine environments. The smaller splittings are due to $^2J_{F(ax)F(rad)}$ = 47 Hz, $^2J_{F(ax)F(rad)'}$ = 83 Hz, and $^2J_{F(rad)F(rad)'}$ = 55 Hz. The vertical intensity scale is arbitrary in each section.

Similar low-frequency chemical shifts for phosphorus have been observed for other tetrachloro-λ^6-phosphoranes, such as the chloroamidino derivatives $Cl_4PN(R)C(Cl)N(R)$ with R = cyclohexyl (-204.7 ppm) and R = isopropyl (-205.2 ppm).[8] The ^{31}P NMR chemical shifts of **1**, **3**, and **7** migrate to lower field

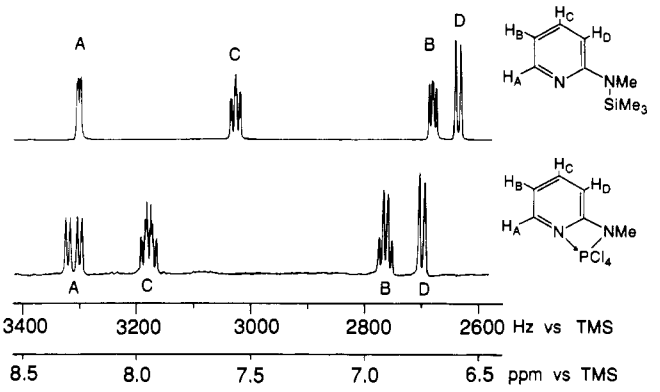

Figure 6. Expansion of the ring-proton region in the ^1H NMR (400 MHz) spectra of (a) 2-(*N*-(trimethylsilyl)-*N*-methylamino)pyridine and (b) **1** at 22 °C.

(higher frequency) as the electronegativity of the substituents increases through the series (E = NPy (-202.2 ppm) < NCH_3 (-195.7 ppm) < O (-184.5 ppm)), showing an increased deshielding of the phosphorus center following the increased electron-withdrawing ability of the atom E in the chelating substituent.

Coupling of the ortho ring proton ($^3J_{PH(A)}$ = 17 Hz) and the amino methyl group ($^3J_{PH(Me)}$ = 27 Hz) in **1** gives an overlapping doublet of quartets in the ^{31}P spectrum. These $^3J_{PH}$ couplings are markedly different from each other and are larger than the usual $^3J_{PH}$ coupling constants.[21] Generally larger values for $^3J_{PH(A)}$ coupling to the ortho ring protons (ranging from 13.6 to 17 for **1-8**) were found in contrast with the much smaller values found in similar compounds such as F_5P·py [6.8 Hz] and F_4P(8-hydroxyquinolyl) (6.0 Hz).[3] In these latter cases, the smaller $^3J_{PH(A)}$ coupling constant could be due to increased electron withdrawal from the P-N bond by either the additional fluorine substituent as in F_5P·py or the larger conjugated ligand system as in F_4P(8-hydroxyquinolyl). The $^3J_{PH(Me)}$ coupling constant of 27 Hz in **1** is also significantly larger than the general range of 4-17 Hz for P-NCH_3 structures and is also larger than the value found in (*N*,*N*'-dimethylchloroamidino)PCl_4 (20.8 Hz)[8] for a very similar interaction. The larger value may reflect in part the increased s character in the bonding through the planar N(2). The smaller coupling observed as triplets in this pattern is residual coupling to other ring protons of the chelate.

The presence of a methyl doublet in the ^1H NMR spectrum of **1** confirms the attachment of the methylamino group to the phosphorus center. The smaller downfield signals due to the ring protons are expanded in Figure 6 wherein strong $^3J_{PH}$ couplings of both the ring proton (H_A) and the methylamino proton (H_{Me}) indicate that both nitrogens are bound to the central phosphorus. Each signal in Figure 6 has been identified through selective decoupling experiments. Comparison of the spectrum of the free 2-((trimethylsilyl)methylamino)pyridine ligand to the chelated ligand in **1** shows clearly the development of the coupling interactions of phosphorus in the bound ligand. It is curious that the J_{PH} couplings are observed for ring protons H_A, H_B, and H_C, but not for H_D, even though H_D is closer to phosphorus by one bond length than is H_C. This pattern may be an indication of withdrawal of electron density from that part of the pyridine ring attached to the methylamino group. A similar pattern was also observed in **3** and **7** (Table III).

The phosphorus NMR signal of **6** (-152.2 ppm) is split into a septet of quartets by fluorine coupling to two different CF_3 groups. Two signals appear in a 2:1 ratio (-67.2 and -62.0 ppm) in the ^{19}F NMR spectrum in the expected doublet of quartets and doublet of septets coupling patterns. The two equivalent CF_3 groups have a larger $^2J_{PH}$ coupling constant (118 Hz) than does the third CF_3 group (91 Hz), and by analogy with $F(CF_3)_3P(O_2CN(CH_3)_2)$,[4a] $CH_3(CF_3)_3P(O_2CN(CH_3)_2)$,[22] and Cl-

(21) Emsley, J.; Hall, D. *The Chemistry of Phosphorus*; Harper and Row Ltd: London, 1976.

$(CF_3)_3PN(R)C(Cl)N(R)$ (R = cyclohexyl)[8] where similar patterns are observed, we deduce that the most appropriate structure is one that contains two axial and one radial CF_3. In all these cases the more intense ^{19}F signal showed the large value of $^2J_{PF}$, so there is an association of larger values of $^2J_{PF}$ with radial positioning of CF_3 groups, which is supported by structure determination.[4a,8,28]

The tetrafluoro analogues (**2**, **4**, **5**, and **8**) can also be identified by their low-frequency ^{31}P NMR chemical shifts (−131.3 to −136.4 ppm), and the shift values are comparable to those for other tetrafluoro-λ^6-phosphoranes, such as F_4P(acac) (−148.7),[1,2] F_4P-(dimethylbenzamidine) (−137.0),[5] and F_4P(8-oxyquinolyl) (−118.7 ppm).[3] The tetrafluoro analogues (**2**, **4**, **5**, and **8**) also displayed the same trend of ^{31}P NMR chemical shift values with respect to the electronegativities of the substituent (E = S (−136.4 ppm) < NPy (−135.2 ppm) < NCH_3 (−132.4 ppm) < O (−131.3 ppm)); thus, both tetrachloro and tetrafluoro groups display similar relative phosphorus deshielding trends according to the E substituent. Other characteristics, such as fluxionality of **2**, **4**, **5**, and **8** discussed below, can also be linked to relative electron-withdrawing abilities of the E groups on the substituents.

The fluxional behavior of **2** and **4** can be associated with rapid exchange of the fluorine atoms at room temperature. Similar fluxional behavior has been observed in the λ^6-(carbamato)-phosphoranes, which also have a four-membered chelating ring, and the behavior was attributed to the opening of this strained four-membered ring to form a pseudorotating pentacoordinate phosphorus center.[4b]

The ^{31}P NMR signals in **2** and **4** appear as pentets of relatively broad lines at ambient temperatures. Although the exchange in **4** could not be "frozen out", the limiting ^{31}P NMR spectrum for **2**, a resolved doublet of doublets of triplets, was obtained (Figure 3) at −50 °C. This splitting pattern indicates the presence of three different fluorine environments around phosphorus in a 1:1:2 ratio, two different radial fluorines (one trans to the ring nitrogen and one trans to the methylamino group) and two equivalent axial fluorines. This assignment is further confirmed by the low-temperature ^{19}F NMR spectrum of **2**, which shows three separate fluorine signals (Table III).

Compounds **5** and **8** did not display fluxional behavior at room temperature, and so structural characterization by NMR spectroscopy was straightforward. The ^{31}P NMR spectrum of **5** (−136.4 ppm (Figure 4)) displays a doublet of doublets of triplets splitting pattern similar to that of **2**, indicating three different fluorine environments in a 2:1:1 ratio. The ^{19}F NMR spectrum of **5** provides confirmation (Figure 5) with three separate fluorine signals. The signal due to the two axial fluorines (−117.8 ppm) shows coupling to phosphorus and to two different radial fluorines. The signals due to each of the radial fluorines (−134.7 and −159.3 ppm) are likewise coupled to phosphorus, the two axial fluorines, and to each other, resulting in a doublet of triplets of doublets. (The signal at −159.3 ppm is slightly overlapped and appears as a doublet of quartets.) Similar patterns are observed for **8** (Table III).

Fluxional Behavior of 2: Barrier to Exchange. Exchange of the fluorine environments at room temperature in **2** was explored by means of two magnetization transfer experiments, spin saturation transfer (SST) and selective inversion transfer (SIT), with the former being the simpler experiment.[14c] These experiments require that the spin–lattice relaxation (T_1) of a nucleus be comparable to its rate of exchange. This applies at 243 K in the case of **2**. Saturation at −69.6 ppm (axial fluorine) of **2** leads to partial saturation transfer of magnetization to the radial fluorines at −72.4 and −88.1 ppm by means of the exchange process. The resultant perturbed integrated signal intensities (the magnitudes of the magnetizations) and independent spin–lattice relaxation (T_1) measurements are combined in eq 1 to give the rate constant (k) for the exchange process. From this rate constant (k) the free energy of activation (ΔG^*) for the fluorine exchange process can be calculated according to eq 2. The result for **2** (56.4 (5) kJ/mol) is almost the same as the ΔG^* value reported previously for the exchange process in $CH_3(CF_3)_3P(O_2CN(CH_3)_2)$ (56 (2) kJ/mol) obtained by line-shape analysis.[4b] Although extensions to other compounds were of interest, the required relation between exchange rate and T_1 hampers generality. In the case of **4**, the exchange was too rapid at all accessible temperatures and the other sites became completely saturated. In the case of **5**, the exchange was too slow and no measurable decrease in signal intensity was observed.

Table VIII. pK_a's of py-E-H, Phosphorus Chemical Shifts, and Fluxionality of Corresponding F_4P Compounds

E	$\sigma(^{31}P)$, ppm	pK_a[a]	rel rate of exchange
O	−131.3	0.75	fast
$N(CH_3)$	−132.4	~6.7 (NH)[b]	*c*
N(py)	−135.2	7.14	
S	−136.4	9.69	slow

[a] Proton loss from the pyridine nitrogen at 20 °C. [b] Value for 2-(methylamino)pyridine was unavailable. The value for 2-aminopyridine is reported. [c] Pseudorotation, $k_1 = 1.87\ s^{-1}$; rotation, $k_2 = 4.39\ s^{-1}$.

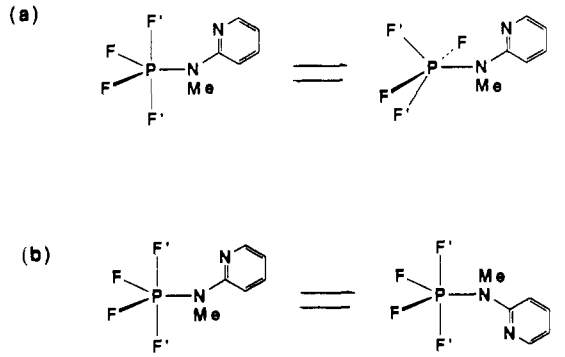

Figure 7. (a) Pseudorotational exchange of axial and radial fluorines in **2**. (b) Ligand rotation (180°) of the monodentate ligand creating exchange of radial fluorines in **2**.

Additional insight into the fluorine-exchange process in **2** was obtained from the selective inversion transfer (SIT) of magnetization experiment in which the change in the magnitude of M_z values for all the three fluorine sites is determined as a function of time. In contrast, the simpler SST experiment measures transfer of saturating z magnetization at only one point in time. The more detailed temporal evolution involved in the SIT experiment provides more detailed information about the exchange process. In the case of **2** under the same temperature conditions the magnetization of one of the radial fluorines (F'_{rad}) at −89.0 ppm was inverted and the z magnetizations (M_z) of the other two sites (F_{ax} and F_{rad}) were observed as a function of time (Table VIII). A modeling program developed by Muhandiram and McClung[14d] was used to compare measured M_z values to simulated M_z values that would be generated by various proposed exchange mechanisms. Because we have no evidence to indicate that six-coordinate twist processes are involved, we have analyzed the processes on the basis of a presumption of a preliminary dissociation of the bidentate chelate to a monodentate substituent to create a fluxional five-coordinate molecule.

One exchange pathway, assigned a rate constant k_1, presumes that the scrambling of fluorines in **2** is due to a Berry[23] pseudorotation process of the five-coordinate phosphorus center (Figure 7a), which results in pairwise interchange of axial and radial fluorines. Another possible exchange mechanism is a simple 180° rotation of the monodentate ligand (Figure 7b), which effectively exchanges only radial fluorines with a rate constant assigned as k_2. The effects of these processes on magnetization transfer rates

(22) Cavell, R. G.; The, K. I.; Vande Griend, L. *Inorg. Chem.* **1981**, *20*, 3813.

(23) Berry, R. S. *J. Chem. Phys.* **1960**, *32*, 933.

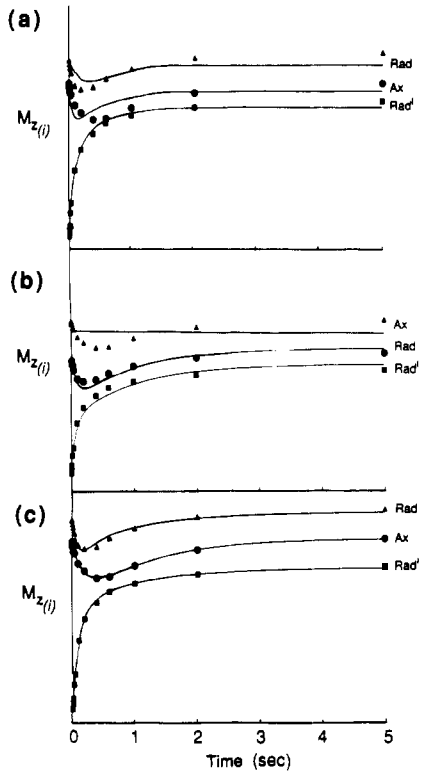

Figure 8. Saturation-inversion-transfer experiment on **2** in $CDCl_3$ solution at −30 °C: (a) solid curves represent behavior calculated for pseudorotation at the λ^5-phosphorus center with $k_1 = 5.76\ s^{-1}$; (b) solid curves represent behavior calculated for rotation of the monodentate ligand only with $k_2 = 5.33\ s^{-1}$; (c) solid curves represent behavior calculated for a combination of pseudorotation ($k_1 = 1.87\ s^{-1}$) and rotation of the monodentate ligand only ($k_2 = 4.39\ s^{-1}$). Magnetizations $M_z(t)$ (arbitrary units) are at the three fluorine sites following a selective inversion of rad' site magnetization. The experimental points are shown for radial (▲), radial' (■), and axial (●) fluorine magnetizations, respectively, in parts a–c.

were calculated and compared to experimental magnetization transfer rates. Pseudorotation alone did not provide good agreement of calculated (solid line) and experimental z magnetization values (▲, ●, ■) (Figure 8a). Similarly, the poor fit of experimental and calculated magnetizations for the rotation-only model (Figure 8b) suggests that ligand rotation alone cannot exclusively account for the observed behavior of the magnetization transfer. A composite model of both motions, ligand rotation and pseudorotation at phosphorus, yielded a good fit (Figure 8c) of experimental and calculated M_z values. Transfer of z magnetization to the radial fluorine is more rapid than transfer to the axial fluorine, and this is reflected in the earlier dip found in the "rad" line compared to the "ax" line shown in Figure 8. The rate constants for the constituent process were determined to be $k_1 = 1.9\ (1)\ s^{-1}$ (pseudorotation at λ^5-phosphorus) and $k_2 = 4.4\ (3)\ s^{-1}$ (monodentate ligand rotation on a λ^5-phosphorus). The corresponding resultant $\Delta G^{\ddagger}$ values are 57.8 (1) for pseudorotation and 56.1 (1) kJ/mol for rotation. The $\Delta G^{\ddagger}$ values are in good agreement with the less specific result given above.

Although it would be interesting to ascertain whether the previously investigated fluorine exchange process in $CH_3(CF_3)_3P(O_2CN(CH_3)_2)$, which shows similar energetic characteristics,[4b] proceeds in a similar fashion, this compound cannot be explored because of the symmetric character of the dimethylcarbamate ligand. Evidence was presented earlier for separable pseudorotation and asymmetric ligand rotation processes in the case of $F_3(CF_3)PSCH_3$[24] (pseudorotation, 54 kJ/mol; ligand (P–S) rotation, 43 kJ/mol). The line-shape analysis procedure used therein however requires a larger difference in the barriers of the component processes whereas the SIT experiments can differentiate between more similar barriers because of the specific focus on magnetization content in particular environments. Unfortunately, T_1 restrictions do not allow universal application of this powerful technique.

The ease of ring opening and consequently the rate of fluorine scrambling in these heteroatom pyridine derivatives of phosphorus(V) increases with the electronegativity of the E substituent (where E = O, NCH_3, NPy, and S), because both the relative exchange rate and the electronegativity follow the trend O > NCH_3 > NPy > S. By drawing electron density away from the pyridine nitrogen to itself, the E substituent reduces the basic character of the pyridine nitrogen and hence its ability to coordinate to the Lewis acid phosphorus center. This weakening of the base–acid interaction increases the rate of fluorine exchange. The influence of the E-group electronegativities is also evidenced by the increased deshielding of the phosphorus chemical shift discussed above. It is noteworthy that the pK_a values[25] of the corresponding free ligand pyridinium ions, which are a reflection of the basicity of the ring nitrogen (eq 8), decrease in the same order and that the more basic ring nitrogen center yields slower fluorine exchange (Table IX).

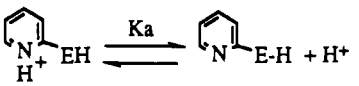

(8)

Conclusion

A new series of neutral hexacoordinate phosphorus compounds (**1–8**) containing strained four-membered rings has been characterized. All possess a characteristic low-frequency ^{31}P NMR chemical shift.

Two compounds (**2** and **4**) displayed fluxional behavior at normal room temperatures comparable to that shown by (dimethylcarbamato)phosphoranes and some amidinophosphoranes, both of which possess four-membered-ring systems incorporating the six-coordinate phosphorus(V) center. A spin-saturation-transfer (SST) experiment gave an energy barrier to the fluorine exchange of 56.4 (5) kJ/mol for compound **2**. The more detailed selective-inversion-transfer (SIT) experiment illustrated that two mechanisms of fluorine exchange are operating in **2** presumably on the dissociated five-coordinate intermediate with energy barriers of 57.8 (1) (pseudorotation) and 56.1 (1) kJ/mol (ligand rotation) at −30 °C. Increasing the electron-withdrawing capability of the pyridine ring substituent at position 2 reduces the basicity of the ring nitrogen, and this leads to the increased rate of fluorine exchange and causes the ^{31}P NMR chemical shift to move downfield.

The X-ray crystal structure of $Cl_4P(map)$ (**1**) shows a hexacoordinate geometry around the phosphorus center in the solid state. The methylamino nitrogen is planar, and with the exception of the methyl hydrogens and the axial chlorines, all the atoms in **1** are coplanar, indicating the formation of a delocalized bidentate anionic structure by the ligand. This ligand system could be systematically modified in many ways to scan an entire spectrum of related chelates with subtle chemical differences. Exploitation of this ligand system to provide a systematic method of exploration of the nature and formation of neutral λ^6-phosphorus compounds would be rewarding.

Acknowledgment. We thank the Natural Science and Engineering Research Council of Canada for financial support. We also thank several of our colleagues at the University of Alberta, Department of Chemistry: Mr. G. Bigam for experimental and Mrs. G. Aarts for computational assistance with the SIT and SST experiments; Professor R. E. D. McClung and Dr. D. R. Muhandiram for access to the computer program for SIT analysis.

(24) Cavell, R. G.; The, K. I.; Gibson, J. A.; Yap, N. T. *Inorg. Chem.* **1979**, *18*, 3400.

(25) (a) Albert, A.; Phillips, J. N. *J. Chem. Soc.* **1956**, 1294. (b) Freier, R. F. *Wässrige Lösungen*; Water de-Gruyter: Berlin, 1975. (c) Anderegg, G. *Helv. Chim. Acta* **1971**, *54*, 509. (d) Albert, A.; Barlin, G. B. *J. Chem. Soc.* **1959**, 2385.

We are indebted to the College of Arts and Science of the University of Toledo for support of the X-ray facility and to F.-P. Ahlers for assistance with the crystallography.

Supplementary Material Available: Tables S1-S6, listing experimental details for the structure determination, thermal parameters, derived hydrogen positions and thermal parameters, and complete bond distances and angles (6 pages); Table S7, listing calculated and observed structure factors (5 pages). Ordering information is given on any current masthead page.

Contribution from the Chemistry Departments, University of Virginia, Charlottesville, Virginia 22901, and North Dakota State University, Fargo, North Dakota 58105

Matrix-Infrared Spectra of Structural Isomers of the Phosphorus Oxysulfide P_4S_3O

Zofia Mielke,[†,‡] Lester Andrews,*[,†] Kiet A. Nguyen,[§] and Mark S. Gordon*[,§]

Received February 5, 1990

Photolysis of the P_4S_3--O_3 molecular complex in solid argon with red light produced two sets of new infrared absorptions including terminal PO and symmetric P-S-P stretching modes, which are assigned to structural isomers of P_4S_3O with terminal oxygen at the apex and base phosphorus positions of P_4S_3. Further ultraviolet photolysis produced evidence for oxo-bridged P_4S_3O and a secondary product, $P_4S_3O_2$.

Introduction

The simplest stable phosphorus sulfide, tetraphosphorus trisulfide, P_4S_3, was discovered by Lemoine in 1864.[1] The bird-cage C_{3v} structure for P_4S_3 has been determined by electron and X-ray diffraction of the vapor and solid phases, respectively.[2,3] According to infrared and Raman spectra of the solid, molten phase, and vapor, P_4S_3 retains the same structure in all three phases.[4] Mass spectra of the vapor show that the molecular ion $P_4S_3^+$ is the most abundant species.[5,6]

Phosphorus oxysulfides are typically prepared by reacting P_4O_{10} or P_4O_6 with P_4S_{10}, which give a range of higher oxysulfides $P_4O_{10-n}S_n$ (n = 2-9).[7,8] However, the oxidation of P_4S_3 in solution with oxygen gas yields a lower oxide of formula $P_4S_3O_4$.[9,10] Matrix reactions with ozone have proven to be a fruitful method for oxidizing phosphorous; red light photolysis of the P_4--O_3 complex in solid argon has produced the terminally bonded P_4O isomer as characterized by infrared spectroscopy.[11,12] An analogous matrix-infrared study of P_4S_3 and O_3 is reported here. Of particular interest is the addition of terminal oxygen to the two different phosphorus positions in the P_4S_3 molecule and the formation of two terminal-oxygen P_4S_3O isomers. To aid in interpretation of the experimental results, electronic structure calculations on P_4S_3O isomers are presented as well.

Experimental Section

The closed-cycle refrigerator, Perkin-Elmer 983 spectrometer, high-pressure mercury arc lamp, vacuum apparatus, and techniques for preparing matrix samples containing ozone have been described previously.[11-13] Ozone was synthesized from normal isotopic, 50% and 98% ^{18}O-enriched oxygen gas. High-resolution infrared spectra were recorded; wavenumber accuracy is ±0.3 cm^{-1}. Tetraphosphorus trisulfide, P_4S_3, obtained from Fluka was evaporated from a quartz or stainless-steel Knudsen cell at 100-110 °C into argon or Ar/O_3 = 150/1 or 75/1 streams and condensed on a cesium iodide window maintained at 12 K. Infrared spectra were recorded, samples were photolyzed with a high-pressure mercury arc (1000 W) using 290-, 420-, and 590-nm glass cutoff and water filters, and more spectra were recorded. After the matrix samples were evaporated, a yellowish white powder, presumably $P_4S_3O_4$, remained on the window.

Electronic structure theory calculations were performed using the effective core potentials[14] recently added to GAMESS.[15] Molecular structures and vibrational frequencies were determined at the self-consistent field (SCF) level of theory, while the final relative energies were obtained with second-order perturbation theory (MP2),[16] at the SCF geometries. For all calculations, a set of six d orbitals was added to each atom, using the exponents from the 6-31G(d) basis sets.[17]

Table I. Infrared Absorptions Produced by Photolysis of P_4S_3--O_3 Samples in Solid Argon at 12 K

group 1		group 2		other	
^{16}O	^{18}O	^{16}O	^{18}O	^{16}O	^{18}O
1218.4	1176.3	1251.0 sh	1207.1 sh	1281.5	1237.5
558.8	557.2	1247.4	1203.9	1262	1219
251.4	248.6	538.3	537.8	753	723
212.3	209.2	500.2	500.0	727	698
		467.5	467.5	523	
		279.3	269.7		

Results

The infrared spectrum of P_4S_3 isolated in solid argon revealed two very strong absorptions at 446 and 429 cm^{-1}, two strong bands at 490 and 224 cm^{-1}, and two medium-intensity bands at 346 and 292 cm^{-1}. These bands are 2-6 cm^{-1} higher than peaks reported for P_4S_3 in a Nujol mull.[4] Photolysis of the matrix sample with 590-1000- and 220-1000-nm radiation for 1-h periods produced no changes in the infrared spectrum.

The codeposited sample containing P_4S_3 and O_3 revealed ozone bands[11] at 1104, 1040, and 704 cm^{-1}, the above P_4S_3 absorptions,

(1) Lemoine, G. *C. R. Hebd. Seances Acad. Sci.* **1864**, *58*, 890.
(2) Akishin, P. A.; Rambidi, N. G.; Ezhov, Yu. S. *Russ. J. Inorg. Chem. (Engl. Transl.)* **1960**, *5*, 358.
(3) Leung, Y. C.; Waser, J.; Van Houten, S.; Vos, A.; Wiegers, G. A.; Wiebenga, E. H. *Acta Crystallogr.* **1957**, *10*, 574.
(4) Gardner, M. *J. Chem. Soc., Dalton Trans.* **1973**, 691.
(5) Penny, G. J.; Sheldrick, G. M. *J. Chem. Soc. A* **1971**, 243.
(6) Muenow, D. W.; Margrave, J. L. *J. Inorg. Nucl. Chem.* **1972**, *34*, 89.
(7) Walker, M. L.; Peckenpaugh, D. E.; Mills, J. L. *Inorg. Chem.* **1979**, *18*, 2792.
(8) Wolf, G.-U.; Meisel, M. *Z. Anorg. Allg. Chem.* **1984**, *509*, 111.
(9) Stock, A.; Friederici, K. *Ber. Dtsch. Chem. Ges.* **1913**, *46*, 1380.
(10) Hoffman, H.; Becke-Goehring, M. Phosphorus Sulfides. In *Topics in Phosphorus Chemistry*; Griffith, E. J., Grayson, M., Eds.; John Wiley and Sons: New York, 1976; Vol. 8, pp 193-271.
(11) Andrews, L.; Withnall, R. *J. Am. Chem. Soc.* **1988**, *110*, 5605.
(12) Mielke, Z.; Andrews, L. *Inorg. Chem.* **1990**, *29*, 2773.
(13) Andrews, L.; Spiker, R. C. *J. Phys. Chem.* **1972**, *76*, 3208.
(14) Stevens, W. J.; Basch, H.; Krauss, M. *J. Chem. Phys.* **1984**, *81*, 6026.
(15) (a) Dupuis, M.; Spangler, D.; Wendoloski, J. J. NRCC Software Catalog Program QG01, 1981. (b) Schmidt, M. W.; Baldridge, K. K.; Boatz, J. A.; Koseki, S.; Gordon, M. S.; Elbert, S. T.; Lam, B. *QCPE* **1987**, *7*, 115.
(16) Pople, J. A.; Binkley, J. S.; Seeger, R. *Int. J. Quantum Chem.* **1976**, *S10*, 1-19.
(17) (a) Hariharan, P. C.; Pople, J. A. *Theor. Chim. Acta.* **1973**, *28*, 213. (b) Gordon, M. S. *Chem. Phys. Lett.* **1980**, *76*, 163. Krishnan, R.; Frisch, M. J.; Pople, J. A. *J. Chem. Phys.* **1980**, *72*, 4244.

[†] University of Virginia.
[‡] On leave from University of Wroclaw, Wroclaw, Poland.
[§] North Dakota State University.

0020-1669/90/1329-5096$02.50/0